

# Temperature-dependent vibrational dephasing: Comparison of liquid and glassy solvents using frequency-selected vibrational echoes

Qing-Hua Xu and M. D. Fayer

*Department of Chemistry, Stanford University, Stanford, California 94305*

(Received 5 March 2002; accepted 17 May 2002)

Frequency-selected vibrational echo experiments were used to investigate the temperature dependences of vibrational dephasing associated with the 0-1 transition of the CO stretching mode of RuTPPCOPy (TPP=5,10,15,20-tetraphenylporphyrin, Py=pyridine) in two solvents: polymethylmethacrylate (PMMA) and 2-methyltetrahydrofuran (2-MTHF). In PMMA, a glass, the echo decay is exponential at all the temperatures studied, and the dephasing rate increases linearly with increasing temperature. In 2-MTHF, there is a change in the functional form of the temperature dependence when the solvent goes through the glass transition temperature ( $T_g$ ). Below  $T_g$ , the dephasing rate increases linearly with temperature, while above  $T_g$ , it rises very steeply in a nonlinear manner. In the liquid at higher temperatures, the vibrational echo decays are nonexponential. A model frequency-frequency correlation function (FFCF) is proposed in which the FFCF differs for a glass and a liquid because of the intrinsic differences in the nature of the dynamics. At least two motions, inertial and diffusive, contribute to the vibrational dephasing in the liquids. The different temperature dependences of inertial and diffusive motions are discussed. Comparison of the model calculations of the vibrational echo temperature dependence and the data show reasonable, but not quantitative agreement. © 2002 American Institute of Physics. [DOI: 10.1063/1.1492280]

## I. INTRODUCTION

In this paper, the results of ultrafast infrared frequency-selected vibrational echo experiments used to study vibrational dynamics and solute-solvent interactions in both the liquid and glassy environments are presented. Vibrational echo experiments examine solute-solvent interactions<sup>1-3</sup> on the ground electronic state potential surface of the solute molecule by measuring the dephasing of a particular vibrational degree of freedom.<sup>4-8</sup> By eliminating inhomogeneous broadening of a vibrational absorption line, vibrational echo experiments are capable of revealing underlying dynamical information that is masked in linear spectroscopic experiments.<sup>3</sup> However, the ultrashort infrared (IR) pulses necessary to study vibrational dephasing in liquids at elevated temperatures have bandwidths that can exceed the anharmonicity of the vibrational transition and the frequency separation between different vibrational transition frequencies. Frequency-selected vibrational echo experiments simplify the study of solute-solvent dynamics by making it possible to observe the dephasing dynamics of a single vibrational transition without sacrificing time resolution.<sup>9-12</sup> Effectively, a multilevel system can be studied as if it were a two-level system, making it possible to perform a more detailed analysis of the data.<sup>12</sup>

Solute-solvent interactions can be studied by nonlinear optical experiments in both the electronic and vibrational regimes. However, molecular vibrations that give rise to vibrational progressions in an electronic absorption spectrum complicate nonlinear experiments involving electronic tran-

sitions. Intramolecular vibrational modes have significant influence on third-order signals.<sup>13,14</sup> The complexity associated with the simultaneous excitation of many vibronic transitions can make it difficult to analyze the results of ultrafast nonlinear experiments on electronic transitions.<sup>13,15</sup>

Echo experiments exploiting vibrational transitions, ultrafast infrared vibrational echo experiments,<sup>4-8</sup> and Raman vibrational echo experiments<sup>16,17</sup> can avoid the difficulties associated with electronic transition based nonlinear spectroscopy. The Raman echo has been used to study vibrational dephasing in liquids.<sup>16,17</sup> With the advent of ultrafast infrared vibrational echo experiments<sup>4</sup> and due to recent developments in the generation of fs IR pulses,<sup>2</sup> IR vibrational echo experiments have become a useful tool for the study of solute-solvent interactions. Vibrational echo experiments have been used to obtain information on liquids,<sup>5,18-20</sup> glasses,<sup>18-20</sup> and proteins.<sup>21-23</sup>

A potential limitation of the vibrational echo technique is that the broad bandwidth of an ultrashort pulse can span both 0-1 and 1-2 vibrational transitions, complicating data analysis.<sup>9-11</sup> Recently, it has been demonstrated that by recording the two-dimensional (2D) time-frequency vibrational echo signal<sup>24</sup> or using frequency-selected vibrational echoes (choosing the proper detection wavelength for the echo signal, equivalent to a slice through the 2D vibrational echo spectrum),<sup>12,25</sup> information can be obtained on the dynamics associated with a single two-level transition modulated by solvent fluctuations without sacrificing time resolution. A great deal of theoretical work is based on such an idealized two-level system.<sup>3,26,27</sup> Therefore, being able to study a mul-

tilevel system as if it were a two-level system is advantageous.

In the following, the frequency-selected vibrational echo technique is applied to the study of the temperature dependence of the vibrational dephasing associated with the 0-1 transition of the CO stretching mode of a metalloporphyrin-CO compound, RuTPPCOPy (TPP = 5,10,15,20-tetraphenylporphyrin, Py = pyridine), in two solvents, polymethylmethacrylate (PMMA) and 2-methyltetrahydrofuran (2-MTHF). PMMA is a polymer glass at all temperatures studied, while 2-MTHF is a glass-forming liquid with its glass transition temperature at 86 K. In contrast to other metal-carbonyl systems that have been studied previously,<sup>19,28,29</sup> this system has a single CO mode that is nondegenerate. Therefore, complications produced by additional line broadening mechanisms arising from degeneracy or mode-mode coupling are avoided. The results show that the temperature dependences of the pure dephasing rates in two solvent environments are very different. A substantial change in the temperature dependence of the pure dephasing is observed upon passing through the glass transition. A model is proposed to explain the data that involves multiple time scales for the solvent modulation of the vibrational transition frequency. Detailed calculations provide a rationalization for the observations in terms of both inertia and diffusive components of the solvent dynamics.

## II. THEORY

The calculation of nonlinear signals in terms of the system's response function has been presented in detail in the monograph by Mukamel.<sup>3</sup> Here only a very brief description is given. The homodyne third-order vibrational echo signal, detected by a slow detector, is given by

$$S(\tau) \propto \int_0^\infty |P^{(3)}(\tau, t)|^2 dt, \quad (1)$$

where the third-order polarization  $P^{(3)}$  is the convolution of the total response function  $R$  with the interacting electric fields, and  $\tau$  is the delay between the pulses.  $R = \sum_i R_i$  contains a contribution from various dynamical processes and different time-ordering terms, which can be represented by double-sided Feynman diagrams.<sup>3,30-32</sup> The  $R_i$  can be calculated through a line broadening function  $g(t)$ . For positive delay times, only two terms contribute to the rephased vibrational echo signal for a two-level system:  $R = R_{00} + R_{11} = 2 \exp[-2g(\tau) - 2g(t) + g(\tau+t)]$ , where  $R_{00}$  and  $R_{11}$  denote the contributions from ground-state bleaching and vibrational excited-state stimulated emission. In this formula, contribution from the vibrational Stokes shift [originating from imaginary part of  $g(t)$ ] is reasonably assumed to be negligibly small, and, therefore,  $R_{00} = R_{11}$ . The vibrational relaxation contribution to vibrational dephasing can be included in the response function  $R$  by multiplying by a factor of  $\exp[-(t+\tau)/2T_1]$ , where  $T_1$  is the vibrational lifetime of level  $v = 1$ . Diagrams with time orderings that do not lead to rephasing and only contribute to the signal at negative delay times and around  $\tau=0$  have been discussed thoroughly in the literature,<sup>3,32</sup> and the discussions will not be recapitulated

here. The  $g(t)$  function can be directly calculated from the frequency-frequency correlation function (FFCF)

$$g(t) = \int_0^t d\tau_1 \int_0^{\tau_1} d\tau_2 \langle \delta\omega_{10}(\tau_2) \delta\omega_{10}(0) \rangle. \quad (2)$$

The FFCF for a vibrational system<sup>33</sup> provides the connection between the physical processes occurring in the sample and the vibrational echo experimental observable. Through the FFCF, detailed models of the nature of the temperature-dependent dynamical processes that produce vibrational dephasing can be tested.

## III. EXPERIMENTAL PROCEDURES

The apparatus for the ultrafast infrared vibrational echo experiments has been described in detail previously.<sup>10</sup> Briefly, tunable mid-IR pulses centered at 1948  $\text{cm}^{-1}$  with a repetition rate of 1 kHz were generated by an optical parametric amplifier pumped with a regeneratively amplified Ti:sapphire laser. The bandwidth and pulse duration of the pulses were 90  $\text{cm}^{-1}$  [full width at half maximum (FWHM)] and 170 fs (FWHM). A 15%/85% ZnSe beam splitter was used to create a weak beam (wave vector  $\mathbf{k}_1$ ) and strong beam (wave vector  $\mathbf{k}_2$ ). The weak beam was delayed with respect to the strong beam by a stepper-motor translation stage. The beams were crossed and focused in the sample to a spot size of 150  $\mu\text{m}$ . The vibrational echo pulse was generated in the phase-matched direction  $-\mathbf{k}_1 + 2\mathbf{k}_2$ . The echo pulse was passed through a monochromator to select the proper observation wavelength, and the signal was measured with a liquid-nitrogen-cooled HgCdTe detector. The pump-probe signal was also dispersed through the monochromator (set to the 0-1 transition frequency) before detection to suppress scattered light. The resolution of the monochromator was set to 2  $\text{cm}^{-1}$ . The pulse energy was  $\sim 3.5 \mu\text{J/pulse}$  (before the beam splitter). Detailed power studies were performed to make sure that there were no higher-order effects and no heating effects.

RuTPPCO, PMMA, methylene chloride ( $\text{CH}_2\text{Cl}_2$ ), and 2-MTHF were purchased from Aldrich. The RuTPPCOPy/2-MTHF solution was prepared by dissolving the RuTPPCO in 2-MTHF and then adding twofold molar excess of pyridine. Pyridine is the fifth ligand on Ru. The optical density (OD) of the CO stretching mode in the 200  $\mu\text{m}$  path length sample cell was of 0.1. The PMMA glass film was prepared by mixing PMMA with a RuTPPCOPy/ $\text{CH}_2\text{Cl}_2$  solution. The solution was spread on a clean glass plate and dried under a closed atmosphere for 2 days. The sample was then placed under vacuum for 1 week to remove the remaining solvent. The thickness of the PMMA film was  $\sim 200 \mu\text{m}$ , and the OD was  $\sim 0.5$  at the absorption maximum. The samples were placed between two  $\text{CaF}_2$  windows in a copper sample cell. The temperature of the sample was controlled with a continuous-flow cryostat and monitored with a silicon diode temperature sensor bonded to the front  $\text{CaF}_2$  window.

## IV. RESULTS AND DISCUSSION

Figure 1 displays the IR absorption spectra of the CO stretching mode of RuTPPCOPy in PMMA and 2-MTHF at

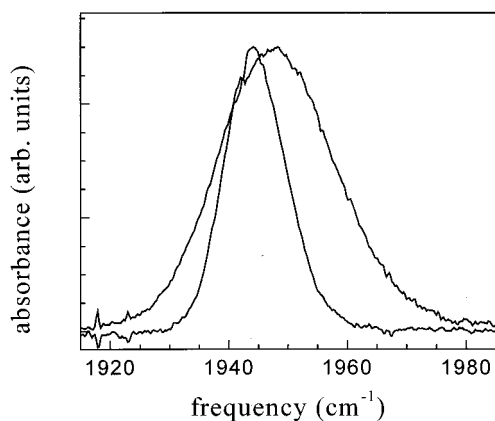


FIG. 1. Absorption spectra of RuTPPCOPy in 2-MTHF (narrow spectrum) and in PMMA (broad spectrum) at 80 K.

80 K. The linewidth in 2-MTHF is significantly narrower than that in PMMA. The absorption spectra in PMMA are Gaussian in shape at all the temperatures studied. In contrast, the spectra in 2-MTHF at low temperatures are Gaussian in shape, but they gain Lorentzian character as the temperature increases. In both solvents, the total absorption line widths are relatively insensitive to the temperature [Fig. 2(a)]. In PMMA, the total linewidth increases slightly as the temperature decreases. In contrast, the linewidth in 2-MTHF is almost temperature independent, showing a slight decrease in width with decreasing temperature that is almost within the experimental error. However, the center transition frequency of CO stretching mode is strikingly different in the two solvents. The center transition frequency in PMMA is temperature independent between 60 K and 320 K [Fig. 2(b)]. In 2-MTHF, the center transition frequency is insensitive to the temperature change below the glass transition temperature, but it increases approximately linearly with increasing temperature above  $T_g = 86$  K [Fig. 2(c)].

The frequency-selected vibrational echo experiments were performed from 60 K to 300 K. Over this range of temperatures, PMMA is a glass, but 2-MTHF goes through its glass transition at 86 K. The detection frequency (monochromator wavelength) was chosen to be on the 0-1 transition but off resonance from the 1-2 transition to avoid multilevel interference effects associated with excitation of the 1-2 transition by the broad bandwidth of the laser pulses.<sup>9,11,12,34</sup> The signal in 2-MTHF was detected at the center frequency of the 0-1 transition. Because the PMMA absorption spectrum is broader, there is spectral overlap between the 0-1 and 1-2 transitions, which can cause oscillations in a 1D echo signal. Therefore, the signal was detected slightly on the blue side of the absorption maximum.<sup>12,25</sup> As has been previously demonstrated experimentally<sup>12,25</sup> and theoretically,<sup>11</sup> at the detection wavelengths used, only the dynamics associated with the 0-1 transition is observed; the measurements at positive times can be modeled as a simple two-level spectroscopic transition.<sup>11,12,25</sup>

The temperature dependences of the dephasing in the two solvent environments are very different. Figure 3 shows the FSVE decay curves at 80, 150 and 250 K. In PMMA, in

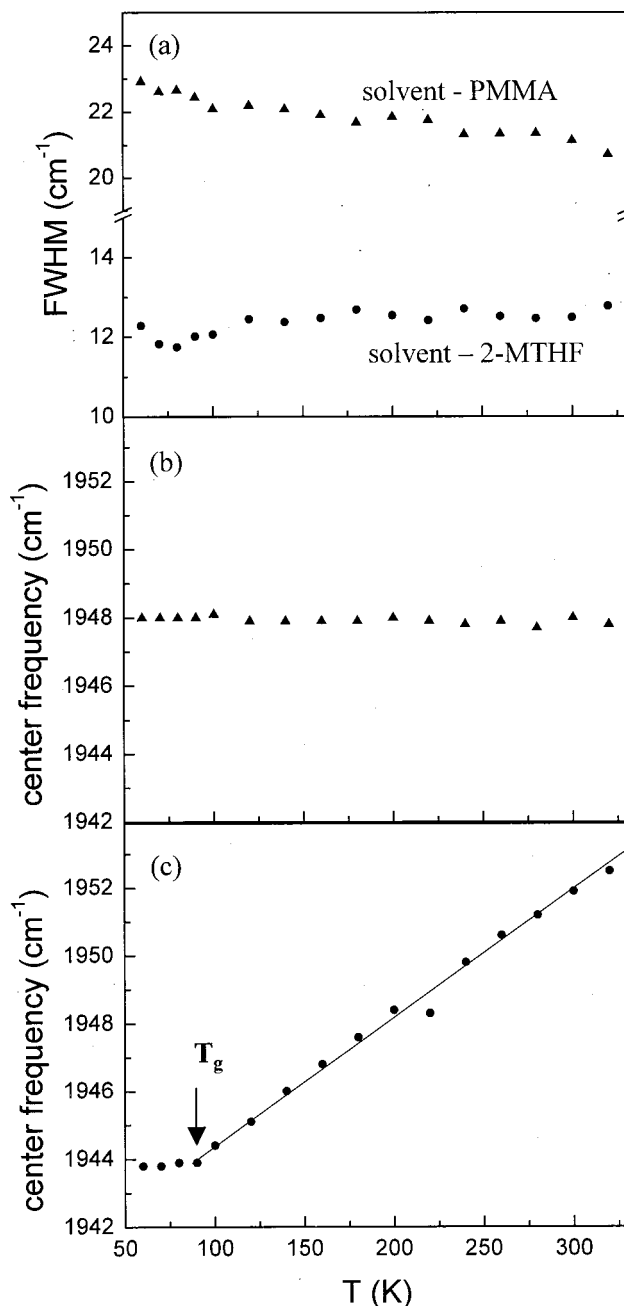


FIG. 2. Temperature dependence of the line width (a) and center transition frequency (b) and (c) of the linear IR absorption spectra of the CO stretching mode of RuTPPCOPy in PMMA (triangles) and 2-MTHF (circles). The line through the data for temperatures above  $T_g$  in (c) is an aid to the eye. The linewidths in both solvents are only slightly temperature dependent. The temperature dependence of the center transition frequency in 2-MTHF shows an abrupt change as the temperature increases above  $T_g$ .

the temperature range 60 to 300 K, all of the echo decays can be fit very well as single exponentials. If the system is in the inhomogeneous broadening limit, then the total dephasing rate is 4 times the echo decay rate, yielding a dephasing time  $T_2$ . Assuming  $T_2$  can be obtained in this manner, the resulting dynamical linewidth ( $1/\pi T_2$ ) is much narrower than the absorption linewidth at all temperatures, which confirms the assumption that the system is in the inhomogeneous limit. The lifetime contribution to the dephasing was removed to obtain the pure dephasing rate using the relation  $1/T_2$

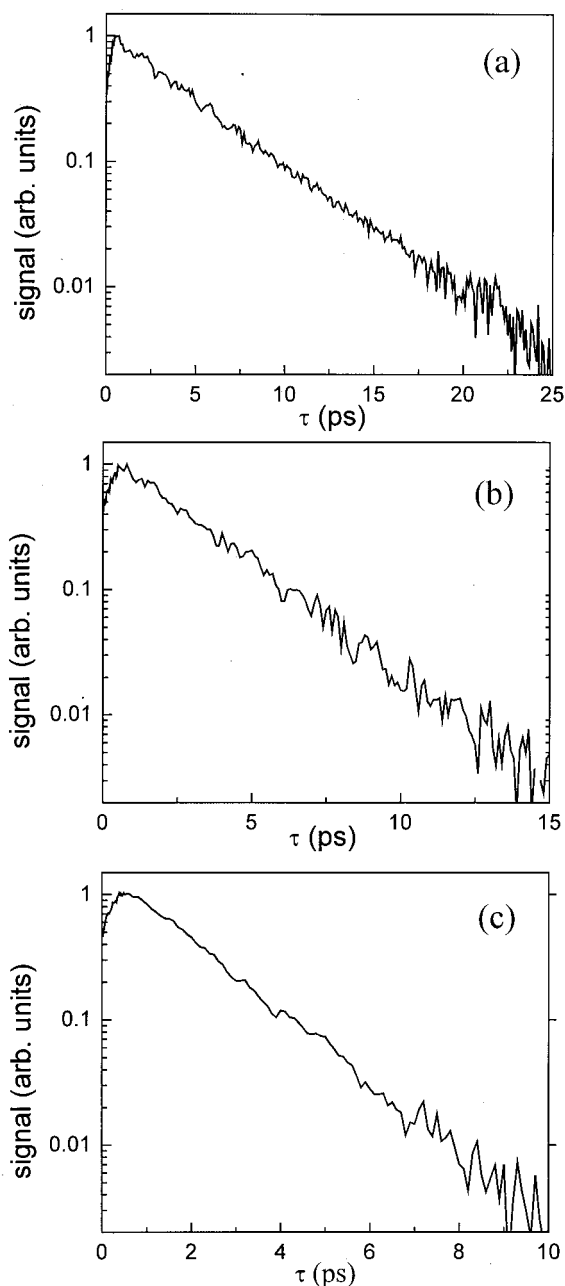


FIG. 3. Frequency-selected vibrational echo decay curves for the CO stretching mode of RuTPPCOPy in PMMA. (a) 80 K, (b) 150 K, and (c) 250 K. The vibrational echo decays are exponential at all temperatures.

$= 1/T_2^* + 1/2T_1$ , where  $1/T_2^*$  is the pure dephasing rate and  $T_1$  is the vibrational lifetime measured with a pump-probe experiment. The vibrational lifetimes in both solvents increase slightly with the increasing temperature, ranging from 12 to 17 ps in the temperature range studied. After the lifetime contribution is subtracted, the pure dephasing rate reflects the dephasing solely induced by dynamic solute-solvent interactions.

The echo decays in 2-MTHF are single exponentials only at low temperatures and become increasingly nonexponential with the increasing temperatures as shown in Fig. 4. Figure 4(a) (60 K) is a single exponential over the full time range. Figure 4(b) (140 K) is exponential except at the shortest times. However, Fig. 4(c) (300 K) is clearly nonexponen-

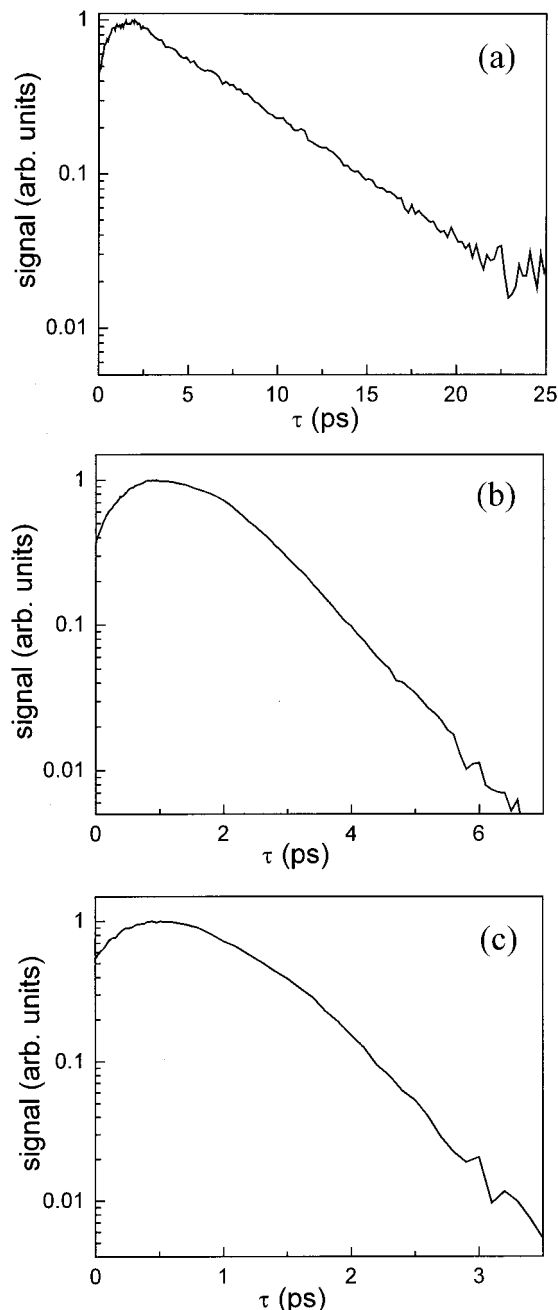


FIG. 4. Frequency-selected vibrational echo decay curves for the CO stretching mode of RuTPPCOPy in 2-MTHF at (a) 60 K, (b) 140 K, and (c) 300 K. The vibrational echo decays are exponential or approximately exponential at lower temperatures ( $\leq 200$  K) and are highly nonexponential at high temperatures.

tial. The dephasing times were extracted by fitting the vibrational echo profiles with single exponentials from 60 to 200 K. The echo decay profiles for temperatures above 200 K are strongly nonexponential, and, therefore, only data for 200 K and below were used here.

The pure dephasing rates in the two solvents are plotted as a function of temperature in Fig. 5. The pure dephasing rate in PMMA (circles) increases linearly with increasing temperature over the full temperature range as is evident from the line drawn through the circles. At the lowest temperatures, the data in 2-MTHF (squares) appear to increase linearly with temperature. The line through the lowest-

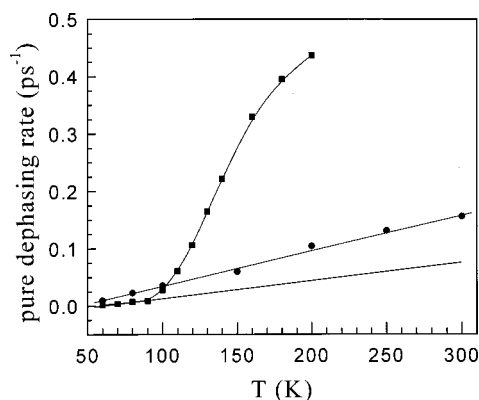


FIG. 5. Temperature-dependent pure dephasing rates of the CO stretching mode of RuTPPCOPy in 2-MTHF (squares) and PMMA (circles). The data taken in PMMA are linear in temperature as shown by the line through the points. In 2-MTHF, for temperatures up to  $\sim T_g$  to ( $T_g = 86$  K), the data are also linear. Above  $T_g$ , the 2-MTHF liquid data become nonlinear and rise steeply. The line through the squares is an aid to the eye.

temperature points is an aid to the eye. However, as the temperature continues to increase, the data rise very steeply. The curve drawn through the points in Fig. 5. is, again, an aid to the eye. At sufficiently high temperatures, the increase becomes somewhat slower. The apparent break in the temperature dependence, from linear to steeply rising nonlinear, occurs just above  $T_g = 86$  K. At the lowest temperatures, where both solvents are glasses, the pure dephasing rates in 2-MTHF are somewhat slower than those in PMMA, and the apparent linear temperature dependence is less steep (see Fig. 5). Thus the homogeneous linewidths in 2-MTHF glass are slightly narrower and increase less rapidly compared to the homogeneous line widths in PMMA in the glassy solvents. In contrast, as the temperature is raised above the 2-MTHF  $T_g$ , the pure dephasing rates in 2-MTHF become much faster than those in PMMA. This fundamental difference in the temperature dependence of the dephasing rates that occurs just above  $T_g$  suggests that an additional dephasing mechanism becomes active when the solvent goes from a solid to a liquid.

In a system studied previously, the asymmetric CO stretching mode of (acetylacetonato)dicarbonylrhodium(I) [Rh(CO)<sub>2</sub>acac] in liquid and glassy dibutylphthalate (DBP),<sup>29</sup> at low temperatures, a linear-in- $T$  dependence was observed. At higher temperatures, the pure dephasing is exponentially activated, and there is no break in the temperature dependence when the solvent passes through  $T_g$ . The exponentially activated dephasing was attributed to the coupling of the CO stretching mode to a low frequency intramolecular mode of Rh(CO)<sub>2</sub>acac.<sup>29</sup>

In the study presented here, the CO stretching mode's vibrational dephasing was studied in two solvents, 2-MTHF, which goes through its glass transition, and PMMA, which does not. The fact that very different temperature dependences are observed in the two solvents and that the dramatic difference turns on when 2-MTHF passes through its glass transition rules out coupling to an intramolecular mode as responsible for the steep temperature dependence observed in 2-MTHF. Instead, the results in the two solvents indicate

that a change in solvent properties that occur around the glass transition temperature is responsible for the onset of the steep temperature dependence that is observed in 2-MTHF liquid. The solvent viscosity changes dramatically as the temperature is raised above  $T_g$  and becomes approximately exponentially activated. Experiments have shown that changes in solvent viscosity can affect vibrational dephasing.<sup>21,22,35</sup> The steep increase in the dephasing rate with increasing temperature observed in 2-MTHF liquid is very likely associated with the temperature dependence of the viscosity as well as the overall temperature change.

When the dynamical contribution to the total absorption spectrum is in the motional narrowing limit, an exponential vibrational echo decay will be obtained either in the homogeneous broadening limit (zero or close to zero inhomogeneous broadening) or in the inhomogeneous broadening limit (a massive amount of inhomogeneous broadening). At low temperatures, when both solvents are glasses, the vibrational echo decays observed in both solvents can be fit well with single exponentials. The measured homogeneous linewidths are much smaller than the corresponding absorption line widths, demonstrating that the absorption spectra are massively inhomogeneous broadened at low temperatures. This is consistent with what might be expected for a solute molecule frozen in a glassy matrix environment. Even in a solid glassy matrix, there are still solvent dynamics. Two types of dynamics can occur. One type is the structural rearrangements that occur in glasses even at low temperatures.<sup>36-38</sup> The second type is phonon-induced dynamics, the so-called "inertial motions." Here we will assume that the inertial motions are solely responsible for the homogeneous dephasing in the glassy state. The semiquantitative agreement between the data and the calculations presented below lends support to this assumption.

Vibrational and electronic transitions of solute molecules in solvents share similar solute-solvent interactions. Although electronic absorption lines are typically one to two orders of magnitude broader than vibrational lines, both electronic and vibrational absorption line shapes in condensed phases are caused by the modulation of transition frequencies by solvent structural variations, which may be dynamic or static. In the context of nonlinear spectroscopy, the dynamic contribution to the line shape or time-dependent observable is produced by the solvent reorganization necessary to accommodate dipole moment (or high-order moment) change or structural change in going from the ground state to the excited state (electronic or vibrational). Both electronic and vibrational dephasings have been studied in liquids.<sup>1,3,6,26,29,39</sup> In the electronic transition regime, theories, such as the multimode Brownian oscillator (MBO) model,<sup>1,3,39</sup> have been proposed to explain the different solvent-induced phenomena observed in optical nonlinear experiments, assuming multiple-modulation time scales. In the MBO model, the transition frequency modulation by solvent fluctuations is usually described in terms of a frequency-frequency correlation function. The FFCF approach has been used in studies of vibrational dephasing and vibrational echo experiments as well.<sup>16,21,24,33,35,40-43</sup> Vibrational echo experiments have also been described in terms of

the Bloch picture (well-separated time scales for homogeneous and inhomogeneous broadening).<sup>6,26,29</sup> Here we model the vibrational dephasing and the vibrational echo decays in terms of a FFCF with a multiple-time-scale functional form.

In a glass, a simple model for the FFCF can be written as

$$\langle \delta\omega_{10}(t) \delta\omega_{10}(0) \rangle = \Delta_h^2(T) \exp(-t/\tau_h) + \Delta_{in}^2, \quad (3)$$

where  $\Delta_h$  is the range of frequencies sampled by the fluctuations that give rise to the homogeneous dephasing and  $\tau_h$  is the time scale characterizing the fluctuations.  $\Delta_h$  reflects the change in energy associated with fluctuations about an essentially fixed local structure. Like phonons in a crystal lattice, heat will cause displacements of the positions and orientations of the solvent molecules without changing the local structure about which the fluctuations occur.  $\Delta_{in}$  is the spread in frequencies that give rise to the inhomogeneous broadening.  $\Delta_{in}$  is caused by the wide variety of local solvent structures in a glass that remained essentially fixed, even on very long time scales. Because the local structures in a glass are frozen in below  $T_g$ ,  $\Delta_{in}$  is assumed to be temperature independent below  $T_g$ . In the motional narrowing limit, the pure dephasing rate  $1/T_2^* = \Delta_h^2 \tau_h$ , and the echo decay rate is  $4/T_2$ . Here  $T_2^*$  is obtained from the vibrational echo decay by removing the lifetime contribution  $T_1$ . The echo decay and pure dephasing rates are insensitive to the  $\Delta_{in}$  when  $\Delta_{in}$  is much larger than  $\Delta_h^2 \tau_h$ . Both the MBO model<sup>3</sup> and the viscoelastic model<sup>41,42</sup> predict that the fluctuation magnitude squared,  $\Delta_h^2$ , is proportional to the temperature.<sup>3,42</sup> In the high-temperature limit,  $\Delta^2 = (2kT/\hbar)\lambda$ ,<sup>3</sup> where  $\lambda$ , the reorganization energy, is assumed to be independent of temperature. In fact,  $\lambda$  has a mild temperature dependence.  $\lambda$  for electronic transitions in polar liquid solvents has been found to decrease  $\sim 20\%$  when the temperature is raised by 100 K.<sup>44</sup> Here  $\lambda$  for vibrational transitions may also have weak temperature dependence, but here it is sufficient to take it to be temperature independent. Using this form for  $\Delta_h^2$ , the linear temperature dependences of the dephasing rates observed in both PMMA and 2-MTHF below their glass transition temperatures suggest that  $\tau_h$  is insensitive to the temperature change. The model given above also predicts that the slope of dephasing rate versus  $T$  below  $T_g$  is proportional to  $\lambda$ . Differences in  $\lambda$  would account for the fact that the homogeneous linewidths in 2-MTHF are narrower and increase less rapidly than those in PMMA at low temperatures (comparing the slopes of two straight lines in Fig. 5). A temperature-independent  $\tau_h$  is consistent with results obtained by Nagasawa *et al.*,<sup>39</sup> which show that the time scales of the inertial motion in PMMA at low and high temperatures (30 and 300 K) are very similar. Therefore, the linear temperature dependences of the vibrational pure dephasing rates observed in PMMA and 2-MTHF glasses are consistent with the proposition that the homogeneous dephasing is phonon induced: that is, ultrafast inertial motions are responsible for the homogeneous dephasing in the high-temperature glasses.

We also note that the dynamical linewidth and total linewidth have opposite temperature dependences in PMMA. The dynamical linewidth increases linearly with the increasing temperature. In contrast, the total linewidth decreases

slightly as the temperature increases [Fig. 2(a)]. This difference could be accounted for by a slight increase in  $\Delta_{in}$  with decreasing temperature in the glassy state. As noted above, in the motional narrowing limit, the pure dephasing (vibrational echo decay) is insensitive to the value of  $\Delta_{in}$  provided  $\Delta_{in} \gg 1/\pi T_2^*$ .

While glasses undergo structural evolution to some extent, the nature of structural dynamics is fundamentally different in solvents such as 2-MTHF when the temperature is raised above  $T_g$  where they become liquids. In comparison to glasses, liquids have greater compressibility and a much larger change in density with temperature. Of particular importance here, as the temperature is raised above  $T_g$ , diffusive motions of the solvent molecules occur on faster and faster time scales. Solvent molecules can reorganize to accommodate changes in the properties of a solute, such as a change in dipole moment, associated with vibrational excitation. In addition to phonon-induced dephasing, solvent diffusive motions provide a dephasing mechanism that is not available in a glass. Therefore, at least two types of motions, occurring on different time scales, can contribute to the pure dephasing in liquids.  $\Delta_{in}$  of Eq. (3) no longer reflects a purely static contribution to the absorption spectrum. To replicate the diffusive dynamics associated with the solvent structure that is essentially static in the glass, a modified FFCF is used,

$$\langle \delta\omega_{10}(t) \delta\omega_{10}(0) \rangle = \Delta_h^2(T) \exp(-t/\tau_h) + \Delta_{in}^2(T) \exp(-t/\tau_d), \quad (4)$$

where  $\tau_d$  is the time associated with the diffusive dynamics and  $\Delta_{in}^2(T)$  is temperature-dependent in the liquid. This formula reduces to Eq. (3) as  $\tau_d \rightarrow \infty$ , that is, below  $T_g$ , where  $\Delta_{in}^2$  is assumed to be temperature independent.

The temperature dependence of the diffusive motions is different from that of the inertial motion. The fluctuation magnitude squared,  $\Delta_{in}^2$ , is assumed to be proportional to the temperature above  $T_g$ .<sup>3,42</sup> In addition, the correlation time  $\tau_d$  is expected to become shorter as the temperature increases. When the CO stretch is excited, the bond length increases and the dipole moment increases. The coupling of the vibrational transition frequency to the solvent could be through direct density fluctuations<sup>41,42</sup> or coupling to the dielectric properties of the solvent. For CO bound to heme in the protein myoglobin, coupling of the CO frequency to variations in the electric field at the CO through the Stark effect is responsible for changes in the CO transition frequency.<sup>21,24,45–47</sup> In a liquid, the time scales of both structural relaxation and dielectric relaxation have very similar temperature dependences.<sup>48</sup> A simple picture relates both the dielectric relaxation time<sup>48</sup> and structural relaxation to the viscosity as  $\tau_d \propto \eta/T$ . Over the temperature range of the experiments in 2-MTHF liquid, the temperature changes about a factor of 2 while the viscosity changes many orders of magnitude. Therefore, we approximate  $\tau_d \propto \eta$ .<sup>22,42</sup> The temperature thus affects  $\tau_d$  through viscosity  $\eta$ . The temperature dependences of  $\Delta_{in}$  and  $\tau_d$  will significantly affect the dephasing rate.

TABLE I. Correlation time scale  $\tau_d$  at different temperatures.

$T$ (K)	100	110	120	130	140	150	160	200
$\tau_d$	200 $\mu$ s	100 ns	4.0 ns	600 ps	100 ps	40 ps	20 ps	4 ps

Model calculations were performed based on the following inputs.  $\Delta_h^2$  and  $\Delta_{in}^2$  were assumed to be linearly proportional to temperature above  $T_g$  and were obtained using the 80 K data as a reference. At 80 K, the vibrational echo decay is exponential. A value of  $\tau_h = 100$  fs is a typical value found for liquids.<sup>42,49</sup> This value is assumed to hold here and, as discussed above, is also assumed to be temperature independent. Using this value, the vibrational echo decay and the linear absorption spectrum was fit to give  $\Delta_h = 0.265$  ps<sup>-1</sup> and  $\Delta_{in} = 0.95$  ps<sup>-1</sup>. The viscosities of 2-MTHF as a function of temperature were obtained from interpolation of the viscosity data.<sup>50</sup> For the model calculation, the constant relating the linear dependence of  $\tau_d$  on  $\eta$  (Refs. 21 and 22) is assumed to be similar to water: that is, viscosities of  $10^1 - 10^6$  cP correspond to the correlation times of from 2 ps to 200 ns.<sup>21,22</sup> Using these correlation times as a function of viscosity and the 2-MTHF viscosities, the correlation times at different temperatures were determined (see Table I). With these inputs, the temperature dependent FFCF for the 2-MTHF solvent is given by

$$\begin{aligned} \langle \delta\omega_{10}(t) \delta\omega_{10}(0) \rangle = & (0.265 \text{ ps}^{-1})^2 \left( \frac{T}{80} \right) \exp(-t/\tau_h) \\ & + (0.95 \text{ ps}^{-1})^2 \left( \frac{T}{80} \right) \\ & \times \exp \left[ -t / \left( \frac{\eta \times 2 \text{ ps}}{10 \text{ cP}} \right) \right]. \quad (5) \end{aligned}$$

The calculations of the vibrational echo decays using Eq. (5) for the FFCF show that the decays are single exponentials at low temperatures [Fig. 6(a), 110 K] and become nonexponential at high temperatures [Fig. 6(b), 260 K], in accordance with experimental observations. In the temperature range of interest here, the calculated decays were fit with single exponentials. In the calculation, a lifetime  $T_1$  contribution of 20 ps is included in the calculation and then subtracted to obtain the values of the pure dephasing rates. Including  $T_1$  in the calculations does not affect the values of pure dephasing rates. This strategy was taken to mimic the real situation.

Figure 7 displays the calculated temperature dependent pure dephasing rates. Of principal importance here is the fact that many of the qualitative features of the experimentally observed temperature dependence (Fig. 5, squares) are reproduced. At the lowest temperatures, the pure dephasing rate increases linearly with temperature. In a calculation for the PMMA solvent, Eq. (3) is used, and the temperature dependence does not deviate from linearity because the diffusive term is frozen and acts as static inhomogeneity. However, for 2-MTHF, modeled with the FFCF given in Eq. (5), the diffusive motion is not frozen, and when  $\tau_d$  becomes fast, the pure dephasing and vibrational echo decay rates are very

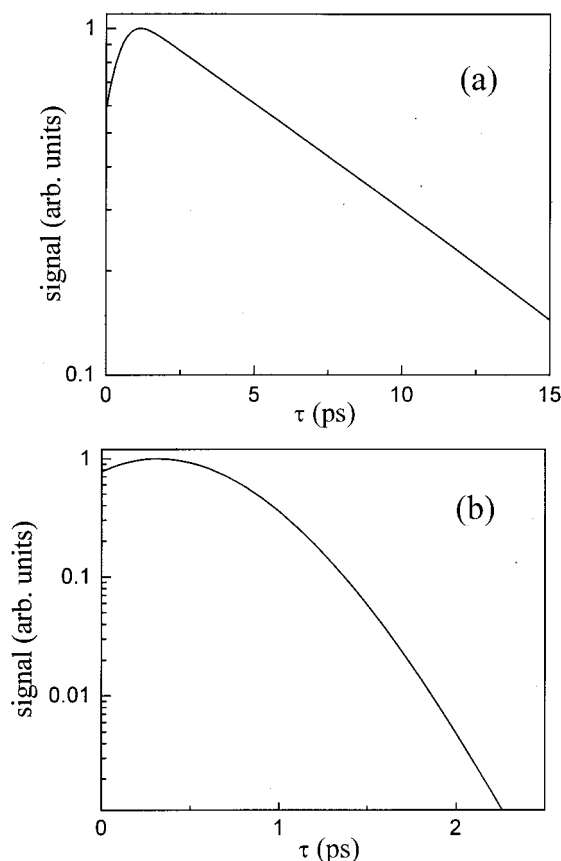


FIG. 6. Calculations of the frequency-selected vibrational echo decay curves using the FFCF of Eq. (5) at (a) 110 K and (b) 260 K. The calculation procedure is described in the text. The vibrational echo decay is exponential at low temperature and nonexponential at high temperature in accordance with the observations in 2-MTHF.

sensitive to the increase in the value of  $\Delta_{in}$ . Above  $T_g$ , the calculated temperature dependence becomes nonlinear, and the rate of pure dephasing increases very rapidly. At sufficiently high temperatures (not investigated here),  $\tau_d$  will be

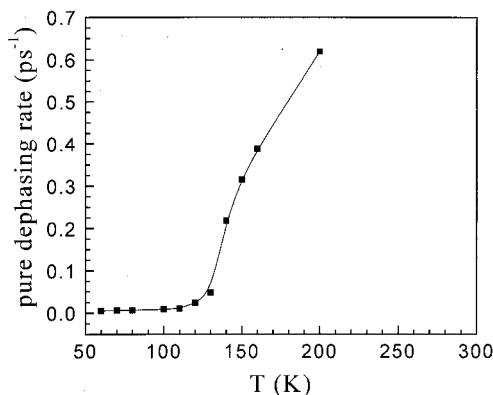


FIG. 7. Model calculations of the pure dephasing rate of the CO stretching mode of RuTPPCOPy in 2-MTHF. The calculations were performed using Eqs. (4) and (5). The calculations reproduce the essential features of the data, but agreement is not quantitative. The calculations are linear in temperature at low temperatures and then rise steeply in the same manner as the data. However, the break from linearity occurs  $\sim 30$  K above  $T_g$ , in contrast to the data that have their break  $< 10$  K above  $T_g$ .

come so fast that the dephasing arising from diffusive motions will also be in the motional narrowing limit ( $\Delta_{\text{in}}\tau_d \ll 1$ ). A pure dephasing rate of  $\Delta_h^2\tau_h + \Delta_{\text{in}}^2\tau_d$  will be obtained, and the corresponding absorption spectrum will be Lorentzian. The reduction in the rate of increase of the dephasing rate with temperature at high temperatures is partially due to the transition from the inhomogeneous broadening limit (the echo decay rate is  $4/T_2$ ) to the homogeneous broadening limit (the echo decay rate is  $2/T_2$ ).

While the calculations based on the FFCF given in Eqs. (4) and (5) capture the main features of the data with no adjustable parameters, the agreement is not quantitative. The focus here is on the vibrational echo decays, but the FFCF can also be used to calculate the linear absorption spectrum. The FFCF shows a mild increase in the width of the absorption spectrum with temperature, which is greater than that seen experimentally. Of particular importance is the fact that the vibrational echo data in 2-MTHF begin to deviate from linearity and rise steeply  $<10$  K above  $T_g$ . In contrast, the calculations do not begin to deviate from linearity and rise steeply until  $\sim 30$  K above  $T_g$ . In addition, the calculated steep increase in the pure dephasing rate with temperature above  $T_g$  is somewhat too steep, and by 200 K it is  $\sim 40\%$  greater than the data value. The actual difference in the magnitude of the pure dephasing is likely due to the use of the relationship between  $\tau_d$  and  $\eta$  based on the approximate values for water. However, the use of a scaling factor between  $\tau_d$  and  $\eta$ , other than the one obtained for water, cannot account for the late onset of the steep rise in the calculated curve. The calculations show that using the FFCF in the form of Eq. (5), the amplitude of  $\Delta_{\text{in}}$  has no effect on the total dephasing rate when  $\tau_d$  is very slow (slower than 1 ns, which is likely for temperatures around  $T_g$ ). However, a possible rapid change of  $\Delta_h$  or  $\tau_h$  just above  $T_g$  would have a large effect on the total dephasing rates and might be responsible for the early onset of the steep temperature dependence observed in the experimental data.

In the model embodied in Eqs. (4) and (5), passage through  $T_g$  was accounted for only by the addition of the viscosity-dependent diffusive dephasing term  $\Delta_{\text{in}}^2 \exp(-t/\tau_d)$ . In the model, the parameters other than  $\tau_d$  were set based on the homogeneous dephasing and the absorption line shape below  $T_g$ . However, when the solvent passes through  $T_g$  from below, there is an abrupt increase in its compressibility.<sup>51</sup> This change could be manifested in an increase in  $\Delta_h$ .<sup>42</sup> In addition, the “softening” of the solvent as it goes above  $T_g$  could cause a change in the “phonon” modes of the solvent, which may well influence the time scale of the inertial response of the system. The glass transition is a very complicated phenomenon, and the nature of the temperature dependence of dynamics in liquids near  $T_g$  is not well understood. Some dynamical processes,<sup>52–54</sup> such as the fast  $\beta$  process (the critical decay in mode coupling theory of supercooled liquids), which has been observed in the Raman and neutron scattering experiments, are not considered in the current model. In the language of mode coupling theory (MCT), the viscosity-dependent structural relaxation corresponds to the  $\alpha$  relaxation.<sup>55</sup> The  $\alpha$  relaxation essentially diverges, becoming extremely slow at the MCT tem-

perature  $T_c$ , which is typically 20% to 30% above  $T_g$ . The calculated curve in Fig. 7 appears as if it corresponds to the onset of fast  $\alpha$  relaxation. The rapid increase observed in the dephasing rate just above  $T_g$  (Fig. 5) provides a new observable for investigation of liquid dynamics near  $T_g$ .

Various possible influences that may result in the abrupt change in the temperature dependence of the pure dephasing above  $T_g$  are currently under investigation. Nonetheless, in spite of the lack of complete quantitative agreement between the data and the model calculations, the calculations capture essential features of the temperature-dependent data.

## V. CONCLUDING REMARKS

The temperature-dependent frequency-selected vibrational echo experiments on the CO stretching mode of RuT-PPCOPy in two solvents PMMA and 2-MTHF (Fig. 5) demonstrate the fundamental difference in the influence of a glassy and a liquid solvent on vibrational pure dephasing. In PMMA, a glass at all temperatures studied, the dephasing rate is linear in temperature. In 2-MTHF, the dephasing is linear for temperatures below  $T_g$ , but it changes form, becoming very steep slightly above  $T_g$ . Calculation using a model frequency-frequency correlation function, which is based on the idea that the same types of solvent dynamics are coupled to vibrational and electronic transitions,<sup>42</sup> show that the different temperature dependences in PMMA and 2-MTHF can be modeled in terms of different FFCF's [Eq. (3) vs Eq. (4)]. Below  $T_g$ , the model describes dephasing in terms of inertial dynamics of the solid. Above  $T_g$ , diffusive motions of the solvent can also contribute to the dephasing. When the system is in the inhomogeneous broadening limit and diffusive processes are frozen out below  $T_g$  [i.e., the FFCF given by Eq. (3)], the pure dephasing is insensitive to the value of  $\Delta_{\text{in}}$ . However, above  $T_g$ , where solvent diffusive motion becomes possible [i.e., the FFCF given by Eq. (4)], the vibrational echo decay becomes very sensitive to the time scale of the diffusive motions,  $\tau_d$ , and to the temperature dependence of  $\Delta_{\text{in}}$ .

Comparison of the temperature dependence of the dephasing rates in PMMA and 2-MTHF supports the picture that at least two different solvent motions contribute to the dephasing in liquids, inertial and diffusive motions. The diffusive motion will be frozen out for glass-forming liquids below their glass transition temperatures, resulting in extensive inhomogeneity. The distinct temperature dependences of the dephasing rates in the two solvents suggest different temperature dependences of the two motions. In the model, the fluctuation magnitude squared for the inertial motion increases linearly with the temperature, while the correlation time scale is insensitive to the temperature. In contrast, in the liquid both the fluctuation magnitude and the correlation time scale of the diffusive motion are dependent on the temperature. The temperature (viscosity dependence) of the time constant of the diffusive motion appears to be at least in part responsible for the activation of the dephasing process above  $T_g$  observed in 2-MTHF. However, the early onset of rapid dephasing just above  $T_g$  suggests that there are additional contributions not contained in the change in viscosity with temperature.

## ACKNOWLEDGMENTS

This work is supported by the fund from National Institutes of Health (Grant No. IR01-GM61137) and the National Science Foundation (Grant No. DMR-0088942). We thank Dr. David E. Thompson and Kusai A. Merchant for their assistance in conducting the experiments.

- <sup>1</sup>C. Rullière, *Femtosecond Laser Pulses: Principles and Experiments* (Springer, Berlin, 1998).
- <sup>2</sup>*Ultrafast Infrared and Raman Spectroscopy*, edited by M. D. Fayer (Marcel Dekker, New York, 2001), Vol. 26.
- <sup>3</sup>S. Mukamel, *Principles of Nonlinear Optical Spectroscopy* (Oxford University Press, New York, 1995).
- <sup>4</sup>D. Zimdars, A. Tokmakoff, S. Chen, S. R. Greenfield, M. D. Fayer, T. I. Smith, and H. A. Schwettman, *Phys. Rev. Lett.* **70**, 2718 (1993).
- <sup>5</sup>A. Tokmakoff and M. D. Fayer, *J. Chem. Phys.* **103**, 2810 (1995).
- <sup>6</sup>K. D. Rector and M. D. Fayer, *Int. Rev. Phys. Chem.* **17**, 261 (1998).
- <sup>7</sup>M. C. Asplund, M. Lim, and R. M. Hochstrasser, *Chem. Phys. Lett.* **323**, 269 (2000).
- <sup>8</sup>M. T. Zanni, M. C. Asplund, and R. M. Hochstrasser, *J. Chem. Phys.* **114**, 4579 (2001).
- <sup>9</sup>K. A. Merchant, D. E. Thompson, and M. D. Fayer, *Phys. Rev. Lett.* **86**, 3899 (2001).
- <sup>10</sup>D. E. Thompson, K. A. Merchant, and M. D. Fayer, *J. Chem. Phys.* **115**, 317 (2001).
- <sup>11</sup>K. A. Merchant, D. E. Thompson, and M. D. Fayer, *Phys. Rev. A* **65**, 023817 (2002).
- <sup>12</sup>Q.-H. Xu, D. E. Thompson, K. A. Merchant, and M. D. Fayer, *Chem. Phys. Lett.* **355**, 139 (2002).
- <sup>13</sup>L. D. Book and N. F. Scherer, *J. Chem. Phys.* **111**, 792 (1999).
- <sup>14</sup>D. S. Larsen, K. Ohta, Q. H. Xu, M. Cyrier, and G. R. Fleming, *J. Chem. Phys.* **114**, 8008 (2001).
- <sup>15</sup>K. Ohta, D. S. Larsen, M. Yang, and G. R. Fleming, *J. Chem. Phys.* **114**, 8020 (2001).
- <sup>16</sup>M. Berg and D. A. Vanden Bout, *Acc. Chem. Res.* **30**, 65 (1997).
- <sup>17</sup>D. A. Vanden Bout and M. Berg, *J. Raman Spectrosc.* **26**, 503 (1995).
- <sup>18</sup>A. Tokmakoff, D. Zimdars, R. S. Urdahl, R. S. Francis, A. S. Kwok, and M. D. Fayer, *J. Phys. Chem.* **99**, 13 310 (1995).
- <sup>19</sup>A. Tokmakoff, D. Zimdars, B. Sauter, R. S. Francis, A. S. Kwok, and M. D. Fayer, *J. Chem. Phys.* **101**, 1741 (1994).
- <sup>20</sup>A. Tokmakoff, R. S. Urdahl, D. Zimdars, R. S. Francis, A. S. Kwok, and M. D. Fayer, *J. Chem. Phys.* **102**, 3919 (1994).
- <sup>21</sup>K. D. Rector, J. Jiang, M. Berg, and M. D. Fayer, *J. Phys. Chem. B* **105**, 1081 (2001).
- <sup>22</sup>M. D. Fayer, *Annu. Rev. Phys. Chem.* **52**, 315 (2001).
- <sup>23</sup>M. C. Asplund, M. T. Zanni, and R. M. Hochstrasser, *Proc. Natl. Acad. Sci. U.S.A.* **97**, 8219 (2000).
- <sup>24</sup>K. A. Merchant, D. E. Thompson, Q.-H. Xu, R. B. Williams, R. F. Loring, and M. D. Fayer, *Biophys. J.* **82**, 3277 (2002).
- <sup>25</sup>Q.-H. Xu and M. D. Fayer, *Laser Phys.* (to be published).
- <sup>26</sup>R. Kubo, in *Fluctuation, Relaxation and Resonance in Magnetic Systems*, edited by D. Ter Haar (Oliver and Boyd, London, 1961).
- <sup>27</sup>R. G. Gordon, *J. Chem. Phys.* **43**, 1307 (1965).
- <sup>28</sup>A. Tokmakoff, B. Sauter, A. S. Kwok, and M. D. Fayer, *Chem. Phys. Lett.* **221**, 412 (1994).
- <sup>29</sup>K. D. Rector and M. D. Fayer, *J. Chem. Phys.* **108**, 1794 (1998).
- <sup>30</sup>Q. H. Xu, G. D. Scholes, M. Yang, and G. R. Fleming, *J. Phys. Chem. A* **103**, 10 348 (1999).
- <sup>31</sup>Q. H. Xu and G. R. Fleming, *J. Phys. Chem. A* **105**, 10 187 (2001).
- <sup>32</sup>T. Joo, Y. Jia, J. Y. Yu, M. J. Lang, and G. R. Fleming, *J. Chem. Phys.* **104**, 6089 (1996).
- <sup>33</sup>D. W. Oxtoby, *Adv. Chem. Phys.* **40**, 1 (1979).
- <sup>34</sup>K. D. Rector, A. S. Kwok, C. Ferrante, A. Tokmakoff, C. W. Rella, and M. D. Fayer, *J. Chem. Phys.* **106**, 10 027 (1997).
- <sup>35</sup>M. A. Berg, K. D. Rector, and M. D. Fayer, *J. Chem. Phys.* **113**, 3233 (2000).
- <sup>36</sup>W. A. Phillips, *J. Low Temp. Phys.* **7**, 351 (1972).
- <sup>37</sup>P. W. Anderson, B. I. Halperin, and C. M. Varma, *Philos. Mag.* **25**, 1 (1972).
- <sup>38</sup>J. T. Fourkas, D. Kivelson, U. Mohanty, and K. A. Nelson, *Supercooled Liquids: Advances and Novel Applications* (American Chemical Society, Washington, D.C., 1997).
- <sup>39</sup>Y. Nagasawa, S. A. Passino, T. Joo, and G. R. Fleming, *J. Chem. Phys.* **106**, 4840 (1997).
- <sup>40</sup>W. G. Rothschild, *J. Chem. Phys.* **65**, 455 (1976).
- <sup>41</sup>M. Berg, *J. Phys. Chem.* **102**, 17 (1998).
- <sup>42</sup>M. A. Berg and H. W. Hubble, *Chem. Phys.* **233**, 257 (1998).
- <sup>43</sup>P. Hamm, M. Lim, and R. M. Hochstrasser, *Phys. Rev. Lett.* **81**, 5326 (1998).
- <sup>44</sup>P. Vath and M. B. Zimmt, *J. Phys. Chem. A* **104**, 2626 (2000).
- <sup>45</sup>E. Oldfield, K. Guo, J. D. Augspurger, and C. E. Dykstra, *J. Am. Chem. Soc.* **113**, 7537 (1991).
- <sup>46</sup>J. D. Augspurger, C. E. Dykstra, and E. Oldfield, *J. Am. Chem. Soc.* **113**, 2447 (1991).
- <sup>47</sup>R. B. Williams, R. F. Loring, and M. D. Fayer, *J. Phys. Chem. B* **105**, 4068 (2001).
- <sup>48</sup>G. Harrison, *The Dynamic Properties of Supercooled Liquids* (Academic, London, 1976).
- <sup>49</sup>S. A. Passino, Y. Nagasawa, T. Joo, and G. R. Fleming, *J. Phys. Chem. A* **101**, 725 (1997).
- <sup>50</sup>A. Tokmakoff, Ph.D. thesis, Stanford University, 1994.
- <sup>51</sup>F. H. Stillinger, P. G. Debenedetti, and S. Sastry, *J. Chem. Phys.* **109**, 3983 (1998).
- <sup>52</sup>V. N. Novikov, *Phys. Rev. B* **58**, 8367 (1998).
- <sup>53</sup>B. Frick and D. Richter, *Science* **267**, 1939 (1995).
- <sup>54</sup>C. A. Angell, *Science* **267**, 1924 (1995).
- <sup>55</sup>G. Hinze, D. D. Brace, S. D. Gottke, and M. D. Fayer, *J. Chem. Phys.* **113**, 3723 (2000).